Cybernetics approaches in intelligent systems for crops disease detection with the aid of IoT

Rajesh Rathinam[1], Padmanathan Kasinathan[2], Uma Govindarajan[3], Vigna K. Ramachandaramurthy[4], Umashankar Subramaniam[5], Susana Garrido[6]

[1]Department of Computer Science and Engineering, Agni College of Technology, Thalambur, Chennai, Tamil Nadu, India

[2]Department of Electrical and Electronics Engineering and Centre for Research and Development, Agni College of Technology, Thalambur, Chennai, Tamil Nadu, India

[3]Department of Electrical and Electronics Engineering, College of Engineering, Guindy, Anna University, Chennai, Tamil Nadu, India

[4]Institute of Power Engineering, College of Engineering, Universiti Tenaga Nasional, Kajang, Malaysia

[5]Department of Communication and Networks, Renewable Energy Lab (REL), Prince Sultan University (PSU), Riyadh, Saudi Arabia

[6]CeBER R&D Center, Faculty of Economics, University of Coimbra, Coimbra, Portugal

Correspondence
Padmanathan Kasinathan, Department of Electrical and Electronics Engineering and Centre for Research and Development, Agni College of Technology, Thalambur, Chennai-600130, Tamil Nadu, India.
Email: padmanathanindia@gmail.com

Abstract

Detection of crop diseases is imperative for agriculture to be sustainable. Automated crop disease detection is a major issue in the current agricultural industry due to its cluttered background. Internet of Things (IoT) has gained immense interest in the past decade, as it accumulates a high level of contextual information to identify crop diseases. This study paper presents a novel method based on Taylor-Water Wave Optimization-based Generative Adversarial Network (Taylor-WWO-based GAN) to identify diseases in the agricultural industry. In this method, the IoT nodes sense the plant leaves, and the sensed data are transmitted to the Base Station (BS) using Fractional Gravitational Gray Wolf Optimization. This technique selects the optimal path for data transmission. After performing IoT routing, crop diseases are recognized at the BS. For detecting crop disease, the input image acquired from the IoT routing phase is then forwarded to the next step, that is, preprocessing, to improve the quality of the image for further processing. Then, Segmentation Network (SegNet) is adapted to segment the images, and extraction of significant features is performed using the acquired segments. The extracted features are adapted by the GAN, which is trained by Taylor-WWO. The proposed Taylor-WWO is newly devised by integrating the Taylor series and WWO algorithms. The

*This is the peer reviewed[1] version of the following article: [*Rathinam R, Kasinathan P, Govindarajan U,Ramachandaramurthy VK, Subramaniam U, Garrido S. Cybernetics approaches inintelligent systems for crops disease detection with the aid of IoT.Int J Intell Syst. 2021*],which has been published in final form at [*https://doi.org/10.1002/int.22560*]. This article may beused for non-commercial purposes in accordance with Wiley Terms and Conditions forUse of Self-Archived Versions.*

proposed Taylor-WWO-based GAN showed improved performance with a maximum accuracy of 91.6%, maximum sensitivity of 89.3%, and maximum specificity of 92.3% in comparison with existing methods.

KEYWORDS
crop disease, generative adversarial network, GLCM features, intelligent systems, internet of things, segmentation network

1 | INTRODUCTION

Artificial intelligence (AI), driven by machine learning (ML) and deep learning, is employed in many applications, including the detection of crop diseases. The agricultural sector is now adopting technological advancement through the Internet of Things (IoT). Cybernetics is a transdisciplinary approach that is applied in complex systems. Cybernetics, a term coined by Novikov,[1] details the history of control methodology logically. Cybernetics deals with models in which a monitor compares and contrasts the present happenings at different sampling times with that of the expected happenings at the same timings. By tracking this behavior, a controller can modify the behavioral patterns of the system accordingly. It is important for cybernetics to operate with core functionalities, such as feedback to understand complex systems. This becomes crucial so that the systems can undergo modifications by themselves based on the environmental response. Jimeneza et al.[2] discussed the comparison of multi-agents and intelligent agent systems in agricultural applications. Figure 1 exemplifies the conceptualization of cybernetics approaches in Intelligent Systems applications.

1.1 | Significance of modernization in agriculture

Trends across the globe are creating an impact on issues, such as poverty, food security, and the overall sustainability of food and agricultural systems. About 58% of the Indian population[6] relies on agriculture as the only source of livelihood.[7] The ministries under the Indian Government, such as the Department of Commerce and the Ministry of Commerce and Industry, have fixed a target for the agricultural sector exports to 60 Billion USD by 2022, as per India Brand Equity Foundation (IBEF). According to the digiteum reports[8,9] and survey,[10] the market for global smart agriculture was estimated at a value of 5098 million USD in the year 2016, and is forecasted to increase up to 15,944 million USD by the end of 2025. This infers that the growth of Compound Annual Growth Rate (CAGR) is more than 13% between 2017 and 2025.[8–10] Figure 2 displays the global population growth.

The economy of an agrarian nation mostly relies on its agricultural productivity. This means that there is a pressing need to understand and analyze disease detection in plants, which is imperative for the growth of agricultural products.[12] The occurrence of diseases is quite natural, and proper care is needed. If proper care is void for plants, it leads to significant and devastating effects on plants, thereby affecting the plant's production and quality. In recent years, the need for automated techniques to detect plant diseases has increased due to growing interest among researchers in agriculture.

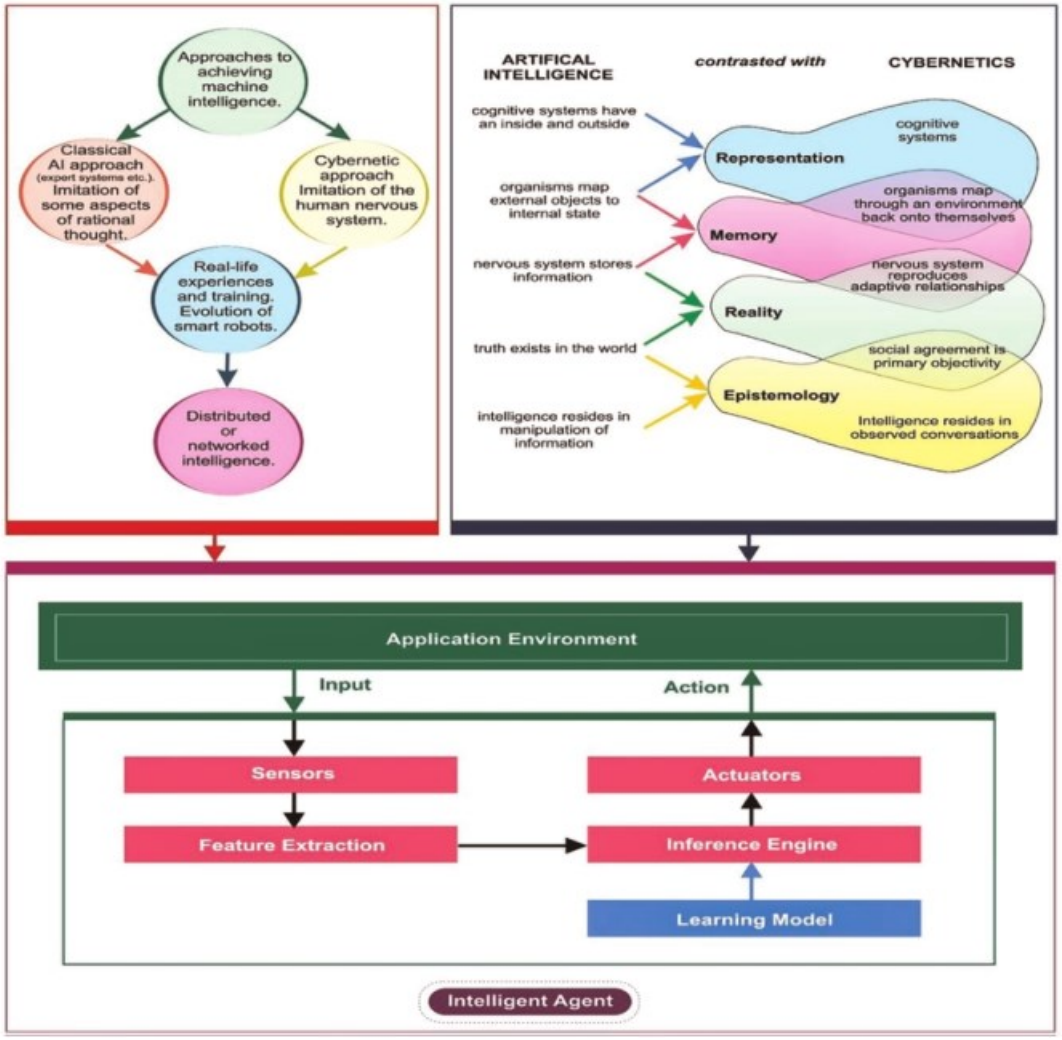

FIGURE 1 Conceptualization of Cybernetics approaches in Intelligent Systems[1,3–5] [Color figure can be viewed at wileyonlinelibrary.com]

Automatic plant disease detection techniques are important as they reduce the need for large-scale monitoring of plant forms and detect diseases at the very beginning when symptoms arise. In this regard, an image segmentation algorithm was developed to detect diseases in plant leaves.[13] The algorithm is an extension of a genetic algorithm wherein the features included were disease detection in leaf, remote monitoring based on server, temperature sensing, sensing of humidity, and moisture sensing. In this paper, sensor-based networks are utilized to measure parameters, such as humidity, moisture, and temperature to automate the process instead of manual checking. Controller-type sensors are also used to control the farm sensors. The camera interfacing technique is used to detect leaf diseases. Wireless Fidelity (WIFI) servers are established at the farmer's receiving end. Sensors detect the status of the farm, leaf diseases' symptoms, and other environmental factors and disseminate information to the WIFI server, which facilitates the farmers to act accordingly.[13–18]

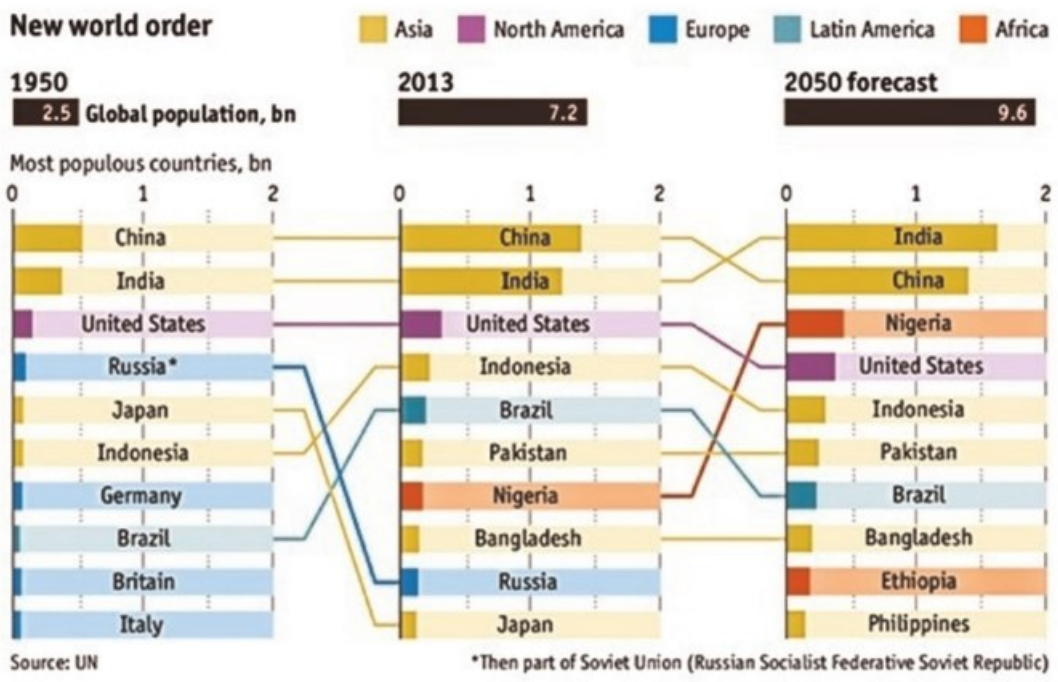

IoT is a promising technology that has gained immense interest amongst researchers due to its ability to perform distributed monitoring in different applications.[19] According to Khatua et al.,[20] IoT has gained more attention these days, thanks to its ability to collect high-level contextual information for the sustainability application. The high-level features effectually detect crop diseases in the wild.[21] With this intellect, the number of sensors and devices used in agricultural domains increased drastically.[22] The materialization of IoT and cloud models is preferred for the overall technological process to decide on agricultural data by the sensors with smart farming.[23]

Both sensors and smart farming techniques leverage information and data technologies to conduct a comprehensive analysis of the farming model. These techniques consider certain factors that involve historical data points before acting on certain functions.[24,25] There exist significant studies and different endeavors to adapt novel IoT technologies to agricultural sectors.[15,26] The determination of crop disease is performed with an IoT-based user-friendly system. IoT brings changes in agricultural industries and enables the farmers to face the issues.[20] The IoT system solves these problems in a significant manner and maximizes the amount of crop production.[15] Figure 3 shows the processes involved in IoT for smart agriculture.

The existing plant disease detection methodologies employed in crop disease detection are discussed herewith their benefits and limitations. A deep learning method, that is, MultiContext Fusion Network (MCFN) was developed to determine the diseases in crops using an IoT network.[21] However, the method failed to use fine-grained identification to detect crop disease. A deep learning method utilized certain factors involving environmental factors and soil fertility to perform crop disease identification.[27] This method effectively handled the soil part using sensors and trained the Convolution Neural Networks (CNN) model. The method improved the overall system's efficiency though it failed to involve

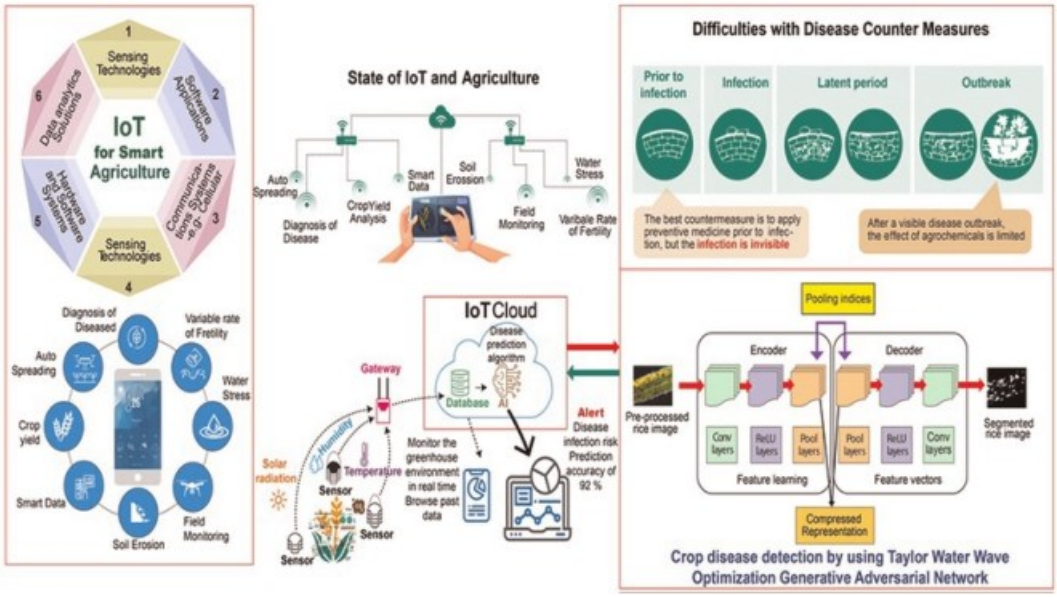

FIGURE 3 IoT framework for smart agriculture and crop disease detection. IoT, Internet of Things [Color figure can be viewed at wileyonlinelibrary.com]

thermal cameras that can sense and predict leaves, whether infected with disease or not. Alonso et al.[24] devised a method, using an agro-industry platform and Global Edge Computing Architecture, to exchange the IoT environmental data to a remote cloud. The goal of the method was to monitor, trace, and optimize the resource to process the chain value in assorted dairy circumstances. However, the method failed to equip consensus algorithms in the detection of possible health issues.

An IoT-based monitoring model for precise agriculture predicts the endemic disease.[19] This monitoring system of agriculture offered monitoring of the environment which maintained a growing atmosphere of crops in optimum grade and predicted the circumstances which result in the outbreak of the disease in an early manner and crop disease detection. Thus, the agricultural monitoring system could store information regarding the environment and soil accumulated from the wireless sensor network. A deep convolutional neural network to categorize rice plants based on the health status of plants diagnosed using images.[28] Here, a three-class classifier was utilized that segregated the status of plant disease as normal, snail-infested plants, or unhealthy plants using the AlexNet deep network. Though the method offered effective performance, it failed to include Leaf Blythe and other rice abnormalities.

A video detection model to identify plant diseases was devised for real-time crop disease and pests.[29] Initially, the video was transformed into still frames. Then the video was fed into a still-image detector for diagnosis. At last, the frames were synthesized in videos. With a still-image detector, a faster-RCNN was utilized to detect the blurred videos. Moreover, video-based evaluation measures using ML classifiers were deployed to detect video quality. The method was applied in other crop diseases and pests. An integrated technique to detect the disease on leaves, that is, Rice Leaf Blast (RLB) was developed based on the image processing method.[30] This method contains a few stages, such as image segmentation, image preprocessing, and image analysis in which the Hue Saturation Value (HSV) color space was utilized. An image

segmentation process was applied to extract the interesting regions, and the patterns were recognized using the MultiLevel Threshold approach. Hence, the severity of RLB disease was classified into three classes: the spreading stage, the infection stage, and the worst stage. An automated diagnosis of crop disease using a prototype model was devised to detect the paddy disease.[31] Here, image recognition was performed to detect the disease and improve the image quality using Twin Support Vector Machine (TSVM) to classify the type of disease in paddy. The method contained four phases: the acquisition of images, preprocessing, image analysis, and classification of diseases in paddy crops. The method attained improved recognition results though it failed to detect other types of diseases.

A Multidimensional Feature Compensation Residual Neural Network (MDFC–ResNet) model was developed to diagnose crop fine-grained disease.[32] This model transmits the diagnostic results to the farmers after the prediction of crop diseases. Also, this model is highly informative in actual agricultural production activities. A disease detection model was developed for plants that function automatically in the IoT environment.[33] In this system, the plant leaf images are captured by placing the nodes in the simulation environment. Aftermath, preprocessing is done for the images captured with the help of a median filter followed by the execution of the segmentation process. Then, the pixel level and segment level features are extracted. Finally, Sine Cosine Algorithm-based rider neural network (SCA-based RideNN) classifies the input to diagnose the disease. This model utilizes minimum resources to identify the plants quickly affected with the disease. However, this method has a disadvantage whereby it fails to identify the sort of plant disease.

Water Wave Optimization (WWO) algorithm was developed to overcome the challenges involved in global optimization.[4] Having been designed as a simple algorithmic framework, WWO can be implemented with ease. With few control parameters in place, WWO can be successfully incorporated with a small-sized population too. The algorithmic framework of WWO is simple and easy to implement and only requires a small-size population and few control parameters. An optimization algorithm named Fractional Gravitational Gray Wolf Optimization (FGGWO) was introduced for energy-efficient routing.[34] The FGGWO is developed by integrating the Gray Wolf Optimization (GWO) and fuzzy gravitational search algorithm (FGSA). In the case of energy and alive nodes, the FGGWO algorithm exhibits excellent performance.

The majority of the imaging methods are devised based on fluorescence and hyperspectral, multispectral, and digital images.[35] In the literary works, the majority of the methods are devised for rice crop disease detection, which includes fuzzy logic,[36] remote sensing, and SVM.[15] In these methods, digital images are usually captured with the help of digital cameras equipped with high resolution. Some of the methods depend on deep learning,[37] particularly CNN, to address the issues of crop disease detection. This scenario proved to exhibit different outperforming automatic identification fields, like, Natural Language Processing and visual recognition.[21,32] Rice disease can affect different parts of the plants. The major infected parts of the plants are the neck node, panicle, and leaf blade.[23,38] From the literary works, the diseases are distinguished. The most number of breaches occurred in the domain of computer vision when DCNN was selected to win the rivalry of Image Net Large-Scale Visual Recognition Challenge (ILSVRC).[21,39] Deep learning seems to be a promising method for tasks related to identification.[40]

The efficiency of CNN is high when it comes to dealing with generic object recognition tasks. This is possible with the help of the deep learning technique, an add-on feature that can identify crop disease since this task suffers from unconvinced performance due to the impact of real-world scenarios.[41] Though different methods are available, for instance, deep learning

mechanisms to identify different crop diseases, like, tomato plant disease, banana leaf disease, and rice disease, researchers turned their spotlight towards the detection of multiclass crop disease concurrently in wild surroundings.[21]

1.2 | Motivation

The Indian economy is dependent on agricultural productivity. Today's advanced technologies enable human society to be self-reliant and produce the required food to meet the ever-growing food demands. Nevertheless, food security remains endangered by various factors, such as climate change, crop diseases, and so on. Crop disease poses a major threat to food security and the livelihood of small-scale farmers who rely completely on farming practices for their life. So it becomes inevitable to identify such diseases and curb their spread at very early stages itself. However, the lack of appropriate infrastructure for proper diagnosis remains a hindrance in this regard. To detect a crop disease in the initial stage, the utilization of automatic disease detection methods is favorable. An assortment of efforts has been taken to ensure there is no crop loss incurred due to diseases.

ML techniques have great potential in terms of increased crop disease recognition rate and accuracy. Accordingly, this paper aims to devise a method using the ML model for detecting crop disease via IoT. Recently, the deep learning-based ML model plays a major role in crop disease detection. Even though different deep learning models, such as Dilated Residual Networks (DRN), Deep Long Short-term Memory (LSTM), and Deep Belief Network (DBN) are available for the various disease classification problems, Generative Adversarial Network (GAN) network played a major role in the plant health monitoring. However, the major issue faced by the GAN network is the training algorithm, which needs to be selected depending on the image characteristics so that the training performance in terms of the loss function can be improved through the improvement of faster convergence.

Hence, an optimization algorithm named Taylor-WWO has been developed to train the GAN. In this study, the crop disease prediction is done by utilizing GAN, which generates samples in parallel. This results in a considerable speed-up in sampling. Also, GAN is trained by the proposed Taylor-WWO algorithm, which inherits the advantages of both the Taylor series and WWO. Hence, the proposed Taylor-WWO algorithm improves the overall classification accuracy of GAN to predict crop diseases.

1.3 | Contribution

The main contribution of this paper is the Taylor-WWO-based GAN. The crop disease detection is performed by the proposed Taylor-WWO-based GAN, in which GAN is trained by the Taylor-WWO, which is made by integrating the Taylor series and WWO.

2 | IOT SYSTEM MODEL

IoT comprises various types of objects in which smart devices are also included. There is an association that exists among these smart devices, which tend to exchange data collected throughout the network with each other.

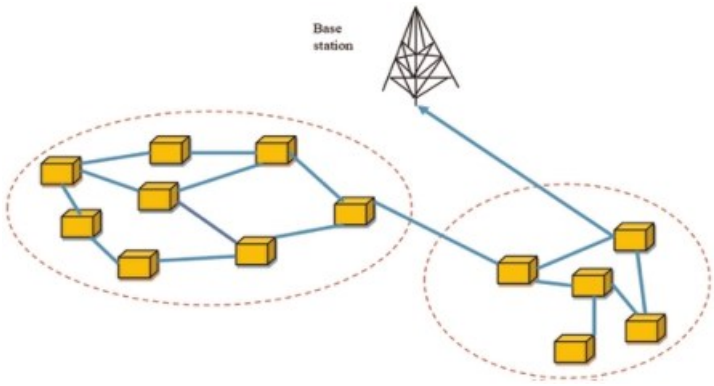

FIGURE 4 System model of IoT network. IoT, Internet of Things [Color figure can be viewed at wileyonlinelibrary.com]

The association of numerous smart devices in the IoT is based on the resources that possess processing and communication potentials to exchange data. Figure 4 represents the components of a typical IoT network and how the system model is a part of it. Here, the network contains numerous nodes which disseminate the data packets to Base Station (BS) by leveraging efficient paths. IoT is spotted in several low-power-consuming networking protocols, for instance, Zwave, 6LoWPAN, and ZigBee. The above-mentioned protocols are developed and focus on specific domains. Since the smart objects remain resource- and energy-constrained, it becomes mandatory for the gateway to be receptive for administration purposes.

Here, an IoT network is assumed in which the number of nodes is designated as g, that is, $G = \{G_1, G_2, \ldots, G_b, \ldots, G_g\}$ and it is encompassed within the coverage area, F . Each IoT node b acquires information related to plant leaves. IoT is essential to enhance production in the agricultural domain, as the IoT nodes can be used for monitoring soil temperature and acidity variables in addition to agricultural variables. Moreover, IoT reinforces the level of productivity, reduces physical work and time, and assists in making the farming procedure a more effective one.

3 | PROPOSED TAYLOR-WWO-BASED GAN FOR CROP DISEASE DETECTION

This section explains the proposed Taylor-WWO-based GAN for detecting crop diseases. The phases involved are the IoT simulation phase, IoT routing phase, and IoT BS phase. Initially, the IoT nodes are subjected to IoT routing. In this phase, IoT routing is carried out based on FGGWO. Once the IoT routing is performed, the crop disease is identified at the IoT BS. The steps followed in the IoT BS are preprocessing, segmentation, feature extraction, and disease detection. The input image acquired from the IoT routing phase is then sent to the next step, that is, preprocessing to enhance the quality of the image for further processing. After preprocessing, segmentation is carried out based on Segmentation Network (SegNet), and in this process, the images are segmented. Then, the feature extraction is performed using texture and statistical features to extract the suitable features for better detection. Finally, the extracted features are utilized, wherein disease detection is carried out using GAN, trained by the proposed optimization algorithm, that is, Taylor-WWO. The proposed Taylor-WWO is a novel

design created by integrating the Taylor series and WWO. Figure 5 displays the crop disease detection model with the proposed Taylor-WWO-based GAN using an IoT network.

Assume a plant disease data set B with c number of images and is expressed as

$$B = \{N_1, N_2, \ldots, N_d, \ldots, N_c\}, \tag{1}$$

where N_d signifies dth input image, and c indicates total images.

Consider that bth IoT node contains the information related to the plant subjected to the routing phase. During this phase, the plant information is transmitted to BS to find the best path using the FGGWO algorithm. A brief description of routing and crop disease detection is given in the subsection below.

3.1 | Routing of sensed information to BS using FGGWO

The next phase is routing, wherein the sensed information is transmitted to BS by choosing the best path using the FGGWO[34] algorithm. Thus, data transmission is performed using the FGGWO algorithm, a combination of GWO and FGSA, to identify the best paths. GWO algorithm works with gray wolves hunting behavior concepts.[41–45] GWO has three major phases: the approaching phase, the hunting phase, and the attacking phase. The search agent's position is generated after the search agents' positions are updated. GWO has a set of four group functions, namely, alpha, beta, delta, and omega. Here, alpha, beta, and delta are deemed to be the fittest solutions. The positions of the search agents are updated by adding the FGSA. On

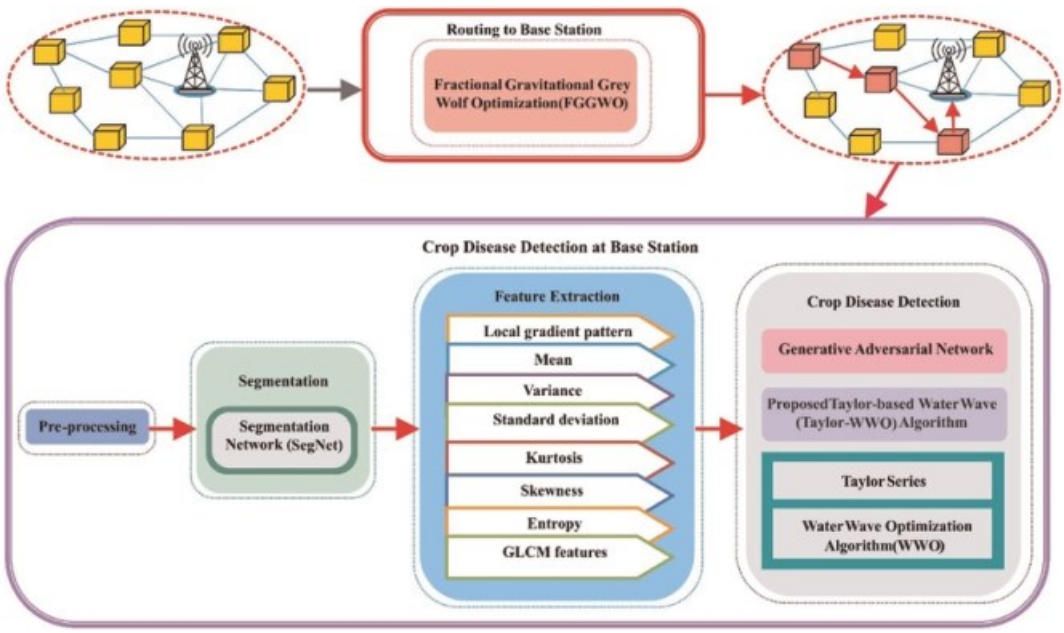

FIGURE 5 Taylor-WWO-based GAN architecture proposed in this study for crop disease detection using IoT network. GAN, Generative Adversarial Network; GLCM, gray-level co-occurrence matrix; IoT, Internet of Things [Color figure can be viewed at wileyonlinelibrary.com]

the basis of FGGWO, the best path is chosen for transmitting the information to the BS. The combined benefits of both the techniques offer numerous paths for transmission using convergence and the capability to function with constraint issues. Here, the update is performed in such a way that the term is added to the GWO algorithm, wherein the added term is based on FGSA. The obtained update equation of FGGWO is expressed as

$$D\,(k+1) = \frac{D_1 + D_2 + D_3 + D_4}{4}, \tag{2}$$

where D_1, D_2, D_3 denote the positions of gray wolves and D_4 indicates the position of FGSA at time k. The representation of each gray wolf position is given as follows.

$$D_1 = D_\alpha - I_1\,(M_\alpha), \tag{3}$$

$$D_2 = D_\beta - I\,(M_\beta), \tag{4}$$

$$D_3 = D_\delta - I_1\,(M_\delta), \tag{5}$$

where D_α, D_β, and D_δ represent the fittest solution, M_α indicates the distance that exists between agent α and the evaluated position, M_β indicates the distance between evaluated position and the agent β, and M_δ indicates the distance that exists between agent δ and the estimated position, and D_4 represents the position of FGSA at the time k and is expressed as follows.

$$D_4 = \gamma C_{ij}\,(k) + K_i\,(k+1) + \frac{\Gamma}{2}\gamma C^{i}_{j}(k-1), \tag{6}$$

where $C_i\,(k)$ represents the position of an agent i at jth dimension in kth time, whereas the agent i's previous position at jth dimension in $(k-1)$th time is denoted by $C_i(k-1)$. Here, $K_i\,(k+1)$ represents velocity at $(k+1)$th time, while γ indicates the real number in the range of 0–1. Thus, the information of plant data obtained from the IoT nodes is given to BS, wherein crop disease detection is done. The steps followed in crop disease detection are described below.

3.2 | Detection of crop disease at BS

The crop disease detected from the agricultural field is exchanged to BS followed by the processes, such as preprocessing, segmentation, and feature extraction. Here, the segmentation is performed using SegNet architecture. The obtained segments undergo significant feature extraction for diagnosing the crop disease. Finally, crop disease detection is performed using GAN that was trained earlier by the Taylor-WWO algorithm proposed in this study. A brief illustration of each process in the detection of plant disease is discussed in the upcoming sections.

3.2.1 | Preprocessing

The preprocessing step is executed to accelerate smooth processing with input plant images. Here, preprocessing is a crucial step in image processing since it makes the images appropriate

for disease detection in crops. In addition, during the preprocessing step, the noise and artifacts in the image are removed. This characteristic is termed as an image enhancement model since it can improve the image contrast for the detection of plant diseases. After the images are preprocessed, it is then subjected to segmentation concurrently to extract significant features, which are apposite for plant disease detection.

3.2.2 | Preprocessed image segmentation for relevant feature extraction

The image obtained after preprocessing is then segmented, for which SegNet[46] is adapted to provide high dimensional segmentation of data. The image that underwent preprocessing comprises various segments, with each one indicating the individual regions. In-plant disease detection strategy, SegNet is adapted to detect the diseased regions considering each segment. Here, the procedure of segmentation for grouping the images, using SegNet, is discussed. Moreover, the decision is taken for each pixel contained in the image. The semantic segmentation technique analyses the images at the pixel level. Furthermore, the model categorizes each pixel based on a predetermined class. SegNet is comprised of an encoder and decoder with a pixelwise layer. Hence, SegNet generates the segments of the preprocessed input image.

Consider the segments generated from the image, which are expressed as

$$S = \{s1, s2, \ldots, se, \ldots, sf\}, \tag{7}$$

where f indicates the total segments present in the image, and s_e is the eth segment of the input image

Figure 6 shows the structural design of SegNet[46] for image segmentation. Here, the encoder is comprised of convolutional layers to perform image segmentation. Hence, the process of training is started from weights that are already trained for classification using large data sets. Each encoder is comprised of the corresponding decoder layer for

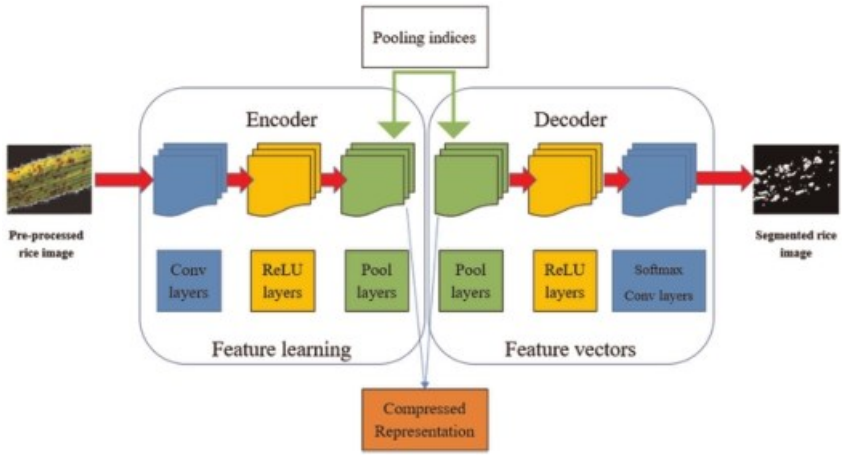

FIGURE 6 SegNet for image segmentation. ReLU, Rectified Linear Nonlinearity; SegNet, Segmentation Network [Color figure can be viewed at wileyonlinelibrary.com]

reconstruction. The output produced by the decoder is then provided to a multiclass softmax classifier to generate the probabilities of class for all the pixels. To produce feature maps set, it becomes a must for every encoder to have convolution and a filter bank. Then, an elementwise Rectified Linear Nonlinearity (ReLU) is adapted while the resulting output is then subsampled. ReLU is utilized to ensure efficiency and rapid connotation of ReLU layer work when a huge network is maintained. In addition, the pool layers minimize the complexity, and there is no weight or bias to train. This is because it processes the inputs in the integration of local regions in the filter. Then, a suitable decoder is adapted to up-sample the input feature maps along with feature maps and learned max-pooling indices. After this, the feature maps are convolved using a trainable decoder filter bank to produce dense feature maps. The output, generated by the final decoder, is then subjected to a soft-max classifier that can be trained. The soft-max classifier segregates every pixel in a sovereign manner. The output generated by the soft-max classifier is L, where L indicates the count of classes. The forecasted segmentation aligns with the class, and it generates the maximal probability in each pixel. Hence, the SegNet is held accountable for producing the segments. SegNet is effectual as it can store the max-pooling indices of feature maps and use it on the decoder to achieve optimal concert.

3.2.3 | Extraction of features using statistical and texture features

After obtaining the segments, the features are extracted using every segment present in the image that underwent preprocessing. The extraction of features certifies effectual plant disease detection in which gray-level co-occurrence matrix (GLCM) features, statistical and texture features are utilized. In case of extraction of the features, every segment is made use of, such that the accuracy in detecting the plant disease gets increased. The features extracted from the segments include GLCM features, texture features, such as Local Gradient Pattern (LGP), and statistical features, which are explained below:

(a) Mean: This value is determined by calculating average pixels present in the image and is formulated as given herewith.

$$T_1 = \frac{1}{|d\,(S_f)|} \times \sum_{f=1}^{|d\,(S_f)|} d\,(S_f), \tag{8}$$

where the total number of segments is denoted by f, the pixel values of each segment is denoted by $d\,(S_f)$, and the whole set of pixels available in the segment is denoted by $|d\,(S_f)|$.

(b) Variance: Variance feature T_2 is computed based on the mean value and is formulated as follows:

$$T_2 = \frac{\sum_{f=1}^{|d\,(S_f)|} |S_f - T_1|}{d\,(S_f)}. \tag{9}$$

(c) Standard deviation: It is a square root of the variance and is symbolized as T_3.
(d) Skewness: Skewness T_4 implies that it illustrates object shape using a numerical value.

(e) Kurtosis: Kurtosis T_5 indicates evenness which describes peak sharpness. Kurtosis indicates the relative peakedness of probability distribution.

(f) Entropy: Entropy[47] is a standard measure that is utilized to discover uncertainty in any data. This measure can be used to maximize mutual information in several functions. The ample accessibility of variations in entropy makes it the right choice for a specific operation. Hence, the entropy of the image is utilized to target the difference that exists between neighbor pixels or pixel groups. In addition, entropy is defined as the corresponding intensity level, which the individual pixels can acclimatize. It is possible to make use of the entropy of image pixels in analytical quantities to compute image details. It offers a better comparison among the details of the image. Hence, entropy is evaluated to obtain the probability and is represented as flows.

$$T_6 = -Q \log(Q), \tag{10}$$

where Q represents the probability distribution of image pixels.

(g) LGP: LGP[48] adapts the value of gradient in eight pixels and is adapted in the current study. The center pixel and gradient values are evaluated using absolute difference, center pixel intensity, and neighboring pixel intensity. The threshold is evaluated as an average of gradient values of the neighboring pixels. Here, the kernel is employed to evaluate the neighbor pixels for the center pixel. After designating the value of a neighboring pixel to be one, the value of the gradient pixel becomes higher than the threshold or otherwise, the value is zero. LGP operator is expressed as

$$T_7^{q,l} = LGP_{\delta,\alpha}^{ul,vl} = \sum^{\beta-1} \eta\,[\bar{\mu}_n - \bar{\mu}^*] \times 2_n, \tag{11}$$

$$\eta\,(s) = \begin{cases} n=0 \\ 0, \ s < 0, \\ 1, \ \text{otherwise}, \end{cases} \tag{12}$$

where μ^* represents the average of gradient values and $\bar{\mu}_n$ signifies the value of gradient among center pixel (λ^*) located at (u_l, v_l) and its neighboring pixels (λ) and is expressed as

$$\bar{\mu}_n = |\lambda - \lambda^*| \,. \tag{13}$$

LGP uses a locally adapted threshold λ^* to generate codes, by initiating the threshold with an absolute intensity difference. LGP produces invariant patterns with gradient differences, and it does not get influenced by variations of local color. The size of color histograms is expressed as [3 × γ] where 'γ' represents bins.

(h) GLCM features: GLCM[45] indicates a second-order efficient statistical feature and is devised by distinguishing the gray-level values for two pixels, using a described spatial location. The combination frequencies of occurrences are evaluated for each gray-level value. GLCM is a two-dimensional array that considers the explicit pixel position based on other pixels.

$$T_8 = P\,(h_1, h_2, \ldots, h_t) = \frac{A_m(h_1, h_2, \ldots, h_t)}{\sum_{Nh-1}^{z1'} \sum_{Nh-1}^{z2} A_m(h_1, h_2, \ldots, h_t)}, \tag{}$$

(14)

where N_h denotes the total number of gray levels in the image, based on tth-order GLCM.

3.2.4 | Construction of feature vector

In Equation (15), a set of features is revealed that include GLCM, statistical features, and texture features. The feature vector is a collection of features, which are extracted from the input data. It is a one-dimensional matrix used to describe features of the input data. The feature vector is formed based on the features, which are useful for the application at hand. Selecting the key features with high predictive value improves the performance of the learning algorithm by enhancing the classification accuracy. Hence, the features acquired from every segment are represented as

$$T = \{T_1, T_2, T_3, T_4, T_5, T_6, T_7, T_8\}, \tag{15}$$

where T represents the feature vector obtained with each segment, T_1 indicates the mean, T_2 indicates the variance, T_3 indicates the standard deviation, T_4 indicates the Skewness, T_5 indicates the kurtosis, T_6 represents the entropy, T_7 signifies the LGP, and T_8 denotes the GLCM features.

Feature vector T is then fed to GAN, which categorizes the input images based on features provided earlier, after which the class label is derived. The plant is segregated by the classifier as either healthy one or infected, equivalent to the input image.

3.2.5 | Detection of crop disease using the proposed Taylor-WWO-based GAN

GAN is a class of AI learning algorithms, which is utilized in unsupervised ML. GAN consists of two neural networks, namely, a generative model and a discriminative model. The internal parameters of a model play a major role in training a model and producing accurate results. This is a reason to use different optimization algorithms to update and calculate appropriate and optimum values of model parameters that influence the learning process and the output of a model. Optimization algorithms are used to train and compile the model of the network. The main purpose of the optimizer is to adjust the weights to minimize errors. Hence, to build efficient and effective models the key is to choose the most appropriate optimization algorithm. Figure 7 describes the workflow of Taylor-WWO-based GAN to detect crop diseases.

Here, the disease is detected using the feature vector obtained earlier. The features extracted in the steps discussed earlier are fed into classification with GAN,[49,50] and the features are trained with the proposed Taylor-WWO, a combination of Taylor series[51] and WWO.[52] The purpose of the proposed Taylor-WWO-based GAN is to detect plant diseases based on the extracted features. Taylor series[51] elaborates the functions of complicated variables and is an extension of a function in an infinite sum of terms. It is a powerful tool, and assists in computing integrals and infinite sums by detecting the Taylor series. In addition, the Taylor series is a one-step procedure that has the potential to handle high-order terms. Taylor series is beneficial for derivations and is utilized to attain hypothetical error bounds. Taylor series facilitates classification accuracy. On the other hand, having been inspired by wave motions, WWO[52] employs three wave-based operators with propagation, refraction, and breaking to enhance a high-dimensional solution space of an optimization issue. The method ensures the balance between exploitation and exploration. In addition, this method increases the convergence process, increases the vibrant nature of the solution, and achieves equilibrium

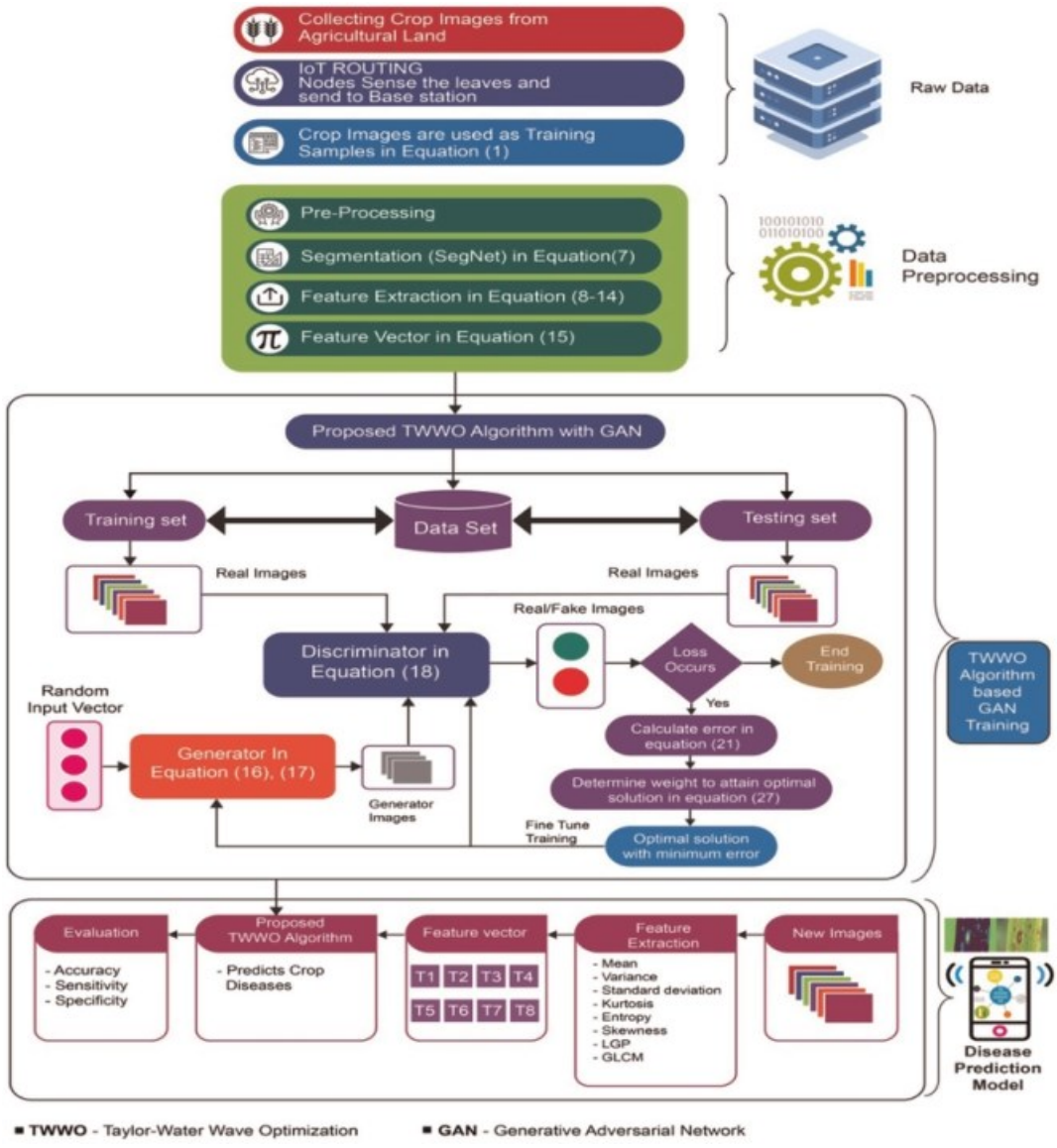

FIGURE 7 Crop disease detection using TWWO-based GAN. GAN, Generative Adversarial Network; GLCM, gray-level co-occurrence matrix; LGP, Local Gradient Pattern; TWWO, Taylor-Water Wave Optimization [Color figure can be viewed at wileyonlinelibrary.com]

between being explored and getting exploited. The authors integrate both WWO and Taylor series to improve the overall performance of the proposed algorithm. The following sections detail the architecture of GAN and its relevant steps.

(i) Structural design of GAN

The feature vector T is fed into GAN to detect plant disease. GAN[49,50] is a deep learning classifier that acquires accurate access when it comes to the detection of plant disease. Most of the time, GAN is leveraged to perform highly precise detection, which brings about a

complex phenomenon. There are two different components present in GAN, such as generator and the discriminator. While the former attempts to create confusion for the latter by producing conceivable data, the latter is generally used to identify fake data in the pool of real data sets. To ensure global convergence, generators, as well as discriminators are made to undergo training in parallel. The generator, present in GAN, is developed based on a full-connected neural network. The data samples are mapped by GAN following prior distribution which in turn is based on the data samples of other such distributions. The plant diseases are accurately detected during the mapping process. Assume the data points as T in which the feature vector is fed as input to GAN. Here, r denotes the high-dimensional random variable while E_{a} corresponds to the distribution of the generative model. Further, the symbol E_{data} denotes real data distribution while a random variable is denoted by E_{o}. In this equation, the generator maps the feature vector T which is represented $G(T)$ in a symbolic fashion. But, the generator function is specifically denoted through $I(\cdot)$ while in case of discrimination function, $J(\cdot)$ denotes the same. Accordingly, the value function $R(J, I)$ is modeled as

$$R(J, I) = U_{O \sim V_{\text{data}}}[\log\ (\ )] + \sim[\log(1 -\ (\ ))], \tag{16}$$

$$R(J, I) = Q_{O \sim V_{\text{data}}}[\log\ (\ )] + \sim[\log(1 -\ (\ (\ ))))]. \tag{17}$$

In the equations, the sigmoid function is denoted by $J(W)$. This is utilized in the computation of probability output to identify renewable energy with the help of a discriminator. Here, $I(w)$ calculates the synthetic information corresponding to distribution. Further, $Q_{I \sim K}$ corresponds to the expectation set by a random variable of data I samples in distribution, K. In this scenario, renewable energy is detected with the help of a discriminator. Further, the modeling of the loss function is performed by the authors using binary classification and cross-entropy. The expression for the loss function of the discriminator is given in the following equation.

$$\hbar_J = -\frac{1}{\vartheta}\sum_{\rho=1}^{\vartheta} G_\rho \log(J(W_\rho)) - \frac{1}{\vartheta}\sum_{\rho=1}^{\vartheta}(1 - G_\vartheta)\log(1 - J(W_\vartheta)). \tag{18}$$

In the equation above, the number of samples is denoted by ϑ. The generator helps in reducing the discriminator gain and is modeled as generator loss function $\hbar_{\text{L}}$, represented as

$$\hbar_{\text{L}} = \max_P R(J, I). \tag{19}$$

GAN is trained using the proposed Taylor-WWO algorithm, after which the crop disease is detected.

(ii) Training of GAN using the proposed Taylor-WWO algorithm

According to Figure 7, the weight of the classifier is made to undergo training with the help of the proposed Taylor-WWO to generate the best solution. Taylor-WWO modifies GAN by combining Taylor series[51] with WWO[52] to select the optimal weights to achieve an update process. For disease detection in the plant, the Taylor-WWO optimization is proposed in this

study. The proposed Taylor-WWO optimization is used to train the weight of the GAN classifier to produce the optimal solution. Through the integration of the WWO and Taylor series, the parametric features of both optimization methods are exploited. This hybrid method increases the performance of classification accuracy. The following is the list of steps for this algorithmic procedure during plant disease detection.

Step 1. Initialization: The foremost step is the initiation of solution and is given as

$$Y = \{Y_1, Y_2, \ldots, Y_v, \ldots, Y_\kappa\}, \quad 1 \le v \le \kappa, \tag{20}$$

where κ represents the total number of solutions and Y_v signifies eth solution

Step 2. Computation of the error: The optimal solution is obtained with error and is modeled as a minimization problem. So, the solution that possesses the least Mean Square Error (MSE) is finalized as the optimal solution. Here is the formulation for MSE.

$$MS_{\text{err}} = \frac{1}{c}\sum_{d=1}^{c} \left\| \xi_d - \xi_d^* \right\|_2 \tag{21}$$

where the expected output is denoted by ξ_d, the predicted output is denoted by ξ^* and c corresponds to the number of data samples, where $1 < d \le c$.

Step 3. Determination of weights: To address the issues of optimization, WWO is employed. As per WWO,[52] the update equation is expressed as

$$Y'_x = Y_x + Rand\,(-1, 1)\lambda X_x, \tag{22}$$

where $Rand\,(-1, 1)$ is the random number, λ indicates the wavelength, and X_x signifies the length of xth search space dimension.

To attain the global optimal solution in plant disease detection, Taylor series[32] is leveraged in the current algorithm. Thus, the updated position of the Taylor series algorithm is given as follows.

$$\begin{aligned} Y'_x = {} & 0.5Y_x + 1.3591Y_x^{y-1} - 1.359Y_x^{y-2} + 0.6795Y_x^{y-3} - 0.2259Y_x^{y-4} \\ & + 0.0555Y_x^{y-5} - 0.0104Y_x^{y-6} + 1.38e^{-3}Y_x^{y-7} - 9.92e^{-5}Y_x^{y-8}, \end{aligned} \tag{23}$$

$$\begin{aligned} Y_x = {} & \left[Y'_x - 1.3591Y_x^{y-1} + 1.359Y_x^{y-2} - 0.6795Y_x^{y-3} + 0.2259Y_x^{y-4} \right] \\ = {} & 2\left[-0.0555Y_x^{y-5} + 0.0104Y_x^{y-6} - 1.38e^{-3}Y_x^{y-7} + 9.92e^{-5}Y_x^{y-8} \right] \\ Y'_x = {} & 2 \end{aligned} \tag{24}$$

Substituting Equation (24) in Equation (22),

$$\begin{aligned} Y'_x = {} & \left[Y'_x \right] - 1.3591Y_{xy-1} + 1.359Y_{xy-2} - 0.6795Y_{xy-3} + 0.2259Y_{xy-4} \\ & - 0.0555Y_x^{y-5} + 0.0104Y_x^{y-6} - 1.38e^{-3}Y_x^{y-7} + 9.92e^{-5}Y_x^{y-8} \end{aligned} \tag{25}$$

$$\begin{aligned} 2_{Y'_x} - {}'_x = {} & 21.3591Y_x^{y-1} - 1.359Y_x^{y-2} + 0.6795Y_x^{y-3} - 0.2259Y_x^{y-4} \\ & + 0.0555Y_x^{y-5} - 0.0104Y_x^{y-6} + 1.38e^{-3}Y_x^{y-7} - 9.92e^{-5}Y_x^{y-8} \end{aligned} \tag{26}$$

The update equation of the proposed Taylor-WWO algorithm is represented as

$$Y'_x = 21.3591 Y_x^{y-1} - 1.359 Y_x^{y-2} + 0.6795 Y_{x-3}^{y} - 0.2259 Y_x^{y-4} + 0.0555 Y_x^{y-5} - 0.0104 Y_x^{y-6} + 1.38 e^{-3} Y_x^{y-7} - 9.92 e^{-5} Y_x^{y-8} \quad (27)$$

TABLE 1 Pseudocode of the proposed Taylor-WWO algorithm

Input: Population $\boldsymbol{P}$ such that $\boldsymbol{Y} = \{\boldsymbol{Y}_1, \boldsymbol{Y}_2, \ldots, \boldsymbol{Y}_v, \ldots, \boldsymbol{Y}_\kappa\}, 1 \cdot \quad v \cdot \quad \kappa$
Output: Best solution Y^*
Begin
Initialize the population of κ solutions in random manner
Compute error using Equation (21)
while stop criteria not satisfied do
for each wave $Y \in P$ do
Propagate Y to new Y' using Equation (22)
if $f(Y') > f(Y)$ then
if $f(Y') > f(Y^*)$ then
Break Y' into waves
Update Y^* with Y'
Replace Y with Y'
Else
$Y.\ell = Y.\ell - 1;$
if $Y.\ell = 0$ then
Refract Y to a new Y' using Equation (27)
Update wavelengths
Compute error using Equation (21)
Return Y^*

Step 4. Error evaluation for update solutions: In this step, the updated solutions' error is analyzed when the weights linked to minimal error are adapted for training GAN.

Step 5. Terminate: Until the optimum weights are attained, the maximum number of iterations is performed. The pseudocode of the proposed Taylor-WWO algorithm is shown in Table 1.

4 | RESULTS AND DISCUSSION

This section presents a detailed note on the evaluation of the proposed strategy against conventional strategies using a rice disease data set based on three parameters, such as accuracy, sensitivity, and specificity. In addition, the energy and throughput plots were drawn by varying the number of iterations. The analysis was conducted by changing the training data percentage. In addition, the authors also analyzed how far the proposed Taylor-WWO-based GAN is effective. The proposed strategy was implemented in MATLAB installed in a PC configured with the Windows 10 operating system, Intel core i3processor, and 2GB RAM. The parameters used for the experimentation: Kernel size—5, activation function—sigmoid, learning rate—0.001, and a maximum number of Epoch—80.

4.1 | Data set description

The analysis was performed using Rice Leaf Diseases data set.[53] This data set contains three classes of diseases, such as bacterial leaf blight, Brown spot, and Leaf smut, with each disease containing 40 images in the JPG format. The characteristic of each data set was multivariate, and the characteristic of the attribute was an integer. The task associated with the data set was classification. The number of instances was 120, and the number of web hits attained 40,468.

4.2 | Performance measures

The efficiency of the proposed Taylor-WWO-based GAN was evaluated using the measures, such as accuracy, sensitivity, and specificity.

4.3 | Experimental results

Figure 8 portrays the experimental results attained from the proposed Taylor-WWO-based GAN using rice plant images. Figure 8A shows the input images obtained from the rice plant image data set, while Figure 8B depicts the preprocessed image obtained from the input image. Figure 8C depicts the ground truth image, whereas the segmented image obtained by SegNet is portrayed in Figure 8D. The LGP extracted image is portrayed in Figure 8E.

4.4 | Performance analysis

This section details the analysis conducted for the proposed Taylor-WWO-based GAN to show its effectiveness in terms of accuracy, sensitivity, and specificity parameters by varying different Epoch and batch sizes.

(a) Analysis by varying Epoch

Figure 9 portrays the analysis of the proposed Taylor-WWO-based GAN after varying Epoch with accuracy, sensitivity, and specificity parameters. The analysis of the proposed Taylor-WWO-based GAN using the accuracy parameter is shown in Figure 9A. In the case of 90% training data, the accuracy value measured by the proposed Taylor-WWO-based GAN with Epoch=2000 was 0.755, Epoch=3000 was 0.854, Epoch=4000 was 0.830, and Epoch=5000 was 0.896.

The analysis of the proposed Taylor-WWO-based GAN using sensitivity parameter is depicted in Figure 9B. In the case of 90% training data, the sensitivity measured by the proposed Taylor-WWO-based GAN with Epoch=2000 was 0.706, Epoch=3000 was 0.756, Epoch=4000 was 0.793, and Epoch=5000 was 0.873. The analysis of the proposed Taylor-WWO-based GAN using specificity parameter is depicted in Figure 9C. In the case of 90% training data, the specificity measured by the proposed Taylor-WWO-based GAN with Epoch=2000 was 0.767, Epoch=3000 was 0.820, Epoch=4000 was 0.780, and Epoch=5000 was 0.877.

(b) Analysis of different batch sizes

In Figure 10, the author portrays the analysis of the proposed Taylor-WWO-based GAN with varying batch sizes using accuracy, sensitivity, and specificity parameters. The analysis of

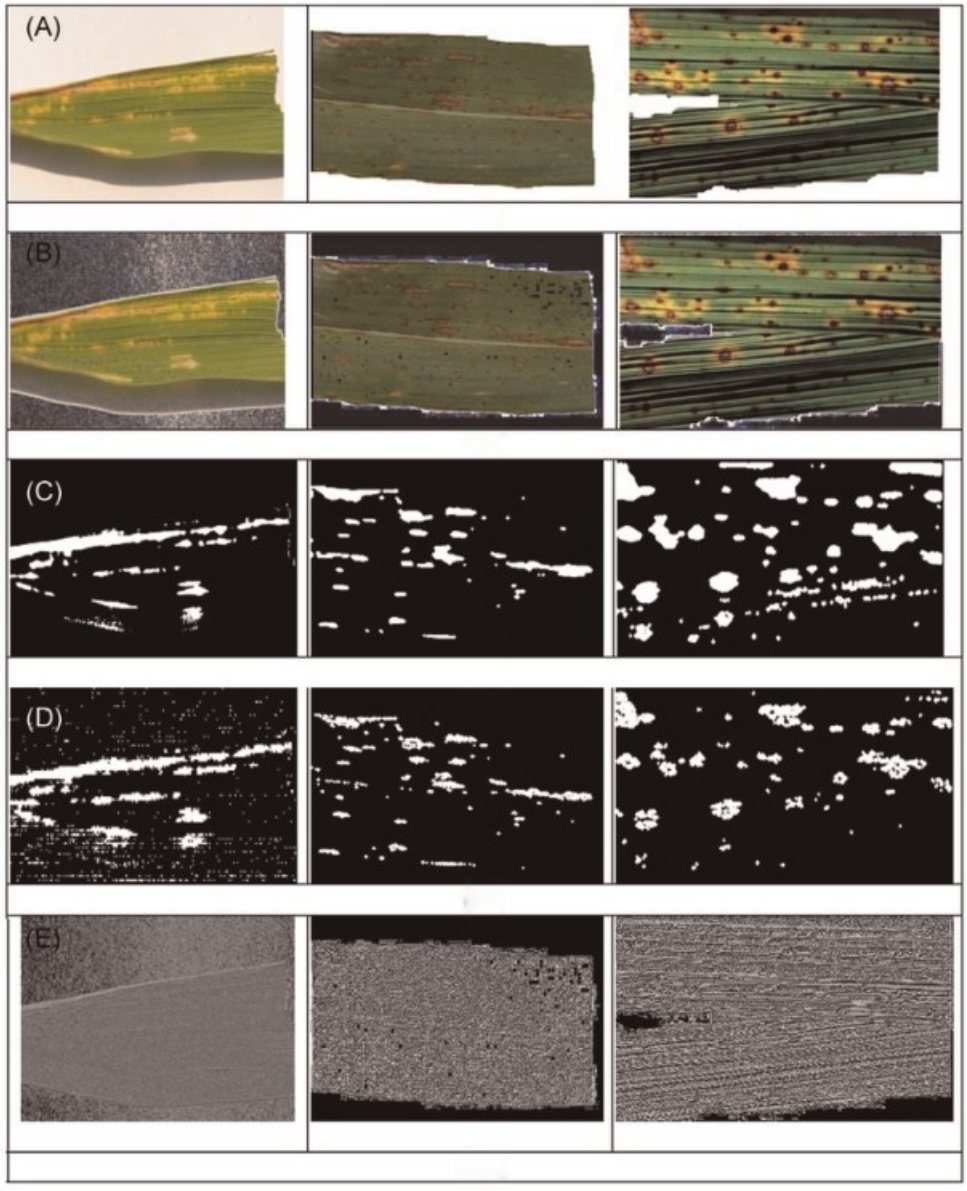

FIGURE 8 Experimental results of the proposed Taylor-WWO-based GAN using: (A) original image, (B) preprocessed image, (C) ground truth, (D) segmented image, and (E) LGP extracted image. GAN, Generative Adversarial Network; LGP, Local Gradient Pattern; WWO, Water Wave Optimization [Color figure can be viewed at wileyonlinelibrary.com]

the proposed Taylor-WWO-based GAN using the accuracy parameter is portrayed in Figure 10A. In the case of 90% training data, the authors measured the accuracy values attained by the proposed Taylor-WWO-based GAN with different batch sizes. The results are as follows: batch size=50 achieved 0.806; batch size=100 attained 0.884; batch size =150 attained 0.798; and batch size =200 accomplished 0.853. The analysis of the proposed Taylor-WWO-based GAN using sensitivity parameter is depicted in Figure 10B.

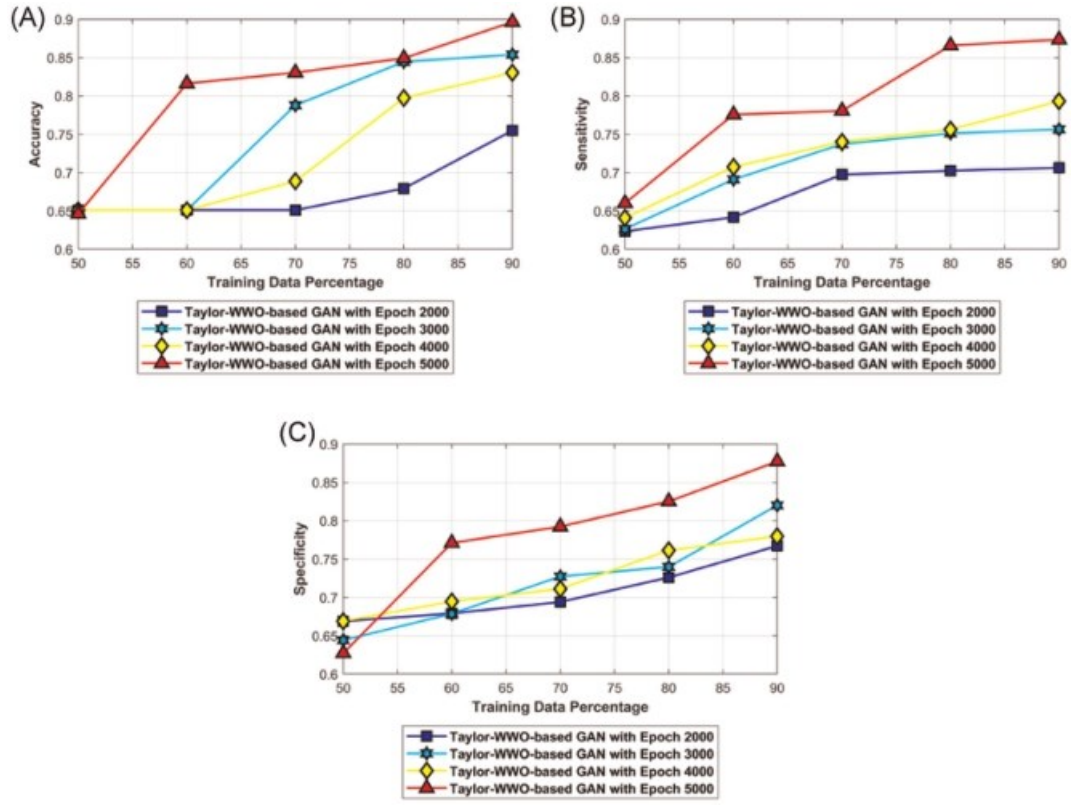

FIGURE 9 Analysis of the proposed Taylor-WWO-based GAN with different Epochs using: (A) accuracy, (B) sensitivity, and (C) specificity. GAN, Generative Adversarial Network; WWO, Water Wave Optimization [Color figure can be viewed at wileyonlinelibrary.com]

In the case of 90% training data, the values of sensitivity measured by the proposed Taylor-WWO-based GAN with batch size=50 was 0.834, and with batch size=100, it was 0.855. In the case of batch size =150, the value was 0.864, and for batch size =200, it was 0.873. The analysis of the proposed Taylor-WWO-based GAN using specificity parameter is depicted in Figure 10C. In the case of 90% training data, the specificity value measured by the proposed Taylor-WWO-based GAN with batch size =50 was 0.853, and for batch size=100, it was 0.814. Likewise, for batch size=150, 0.812 was achieved, and for batch size =200, the value attained was 0.867.

4.5 | Comparative analysis

The authors adapted a few methods to analyze including MCFN,[21] Deep learning-NN,[27] CNN,[23] MDFC–ResNet,[54] SCA-based RideNN,[36] and the proposed Taylor-WWO-based GAN. The methods were analyzed with three parameters, such as accuracy, sensitivity, and specificity as its basis, on different training data. In addition, the energy and throughput were computed on a different number of iterations.

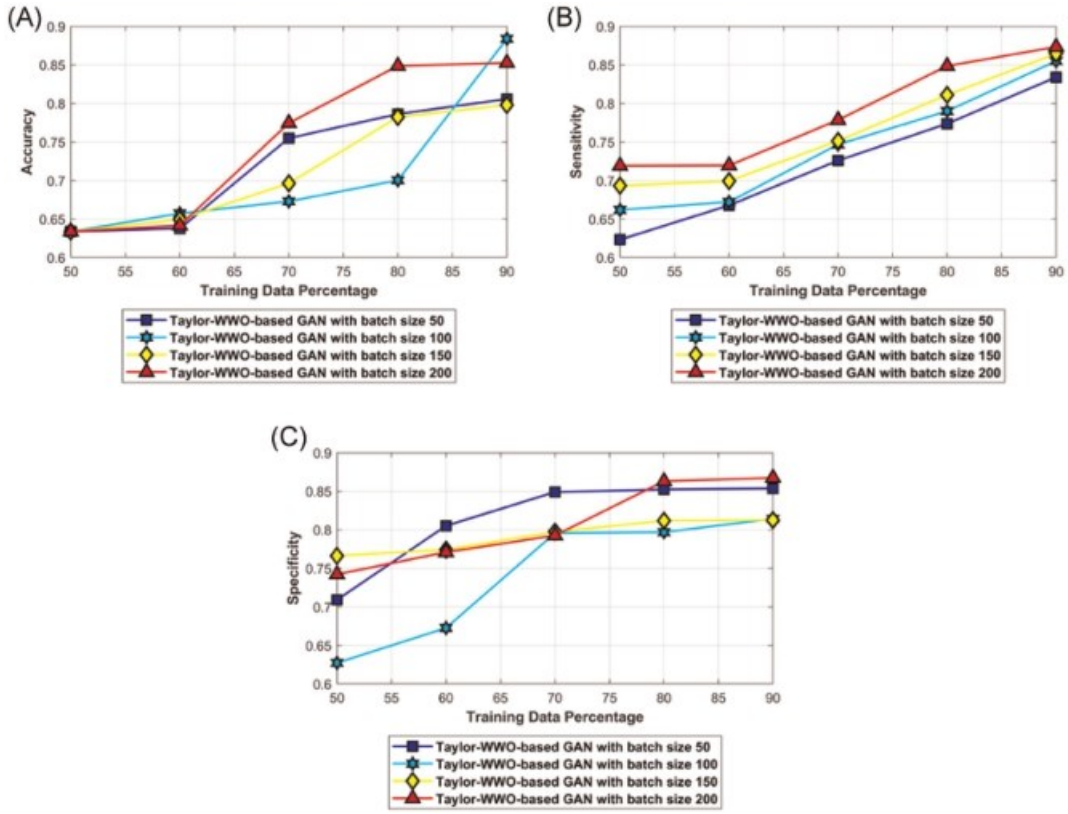

FIGURE 10 Analysis of the proposed Taylor-WWO-based GAN with different batch sizes using: (A) accuracy, (B) sensitivity, and (C) specificity. GAN, Generative Adversarial Network; WWO, Water Wave Optimization [Color figure can be viewed at wileyonlinelibrary.com]

4.5.1 | MCFN

The aim of developing this method is to deploy it in agricultural IoT, especially in recognizing the wild diseases that affect the crop. A standard CNN is first adopted to extract dynamic, unique, and discriminative visual features from 50,000 in-field crop disease samples. Followed by contextual factors are collated as prior information by the image acquisition sensors to help in the classification of crop disease and eventually mitigate the number of false positives. Finally, a deep fully connected network collates contextual features and the visual features to produce the output, that is, correct prediction of crop disease.

4.5.2 | Deep learning NN

This system aims to find out the stress-causing factors among plants, for instance, crop disease, fertility of the soil, and environmental imbalance

4.5.3 | CNN

This system uses image processing techniques and the CNN technique to achieve the key objective, that is, identification of leaf disease and recommend remedies to get rid of the disease.

4.5.4 | MDFC–ResNet

The primary function of this system is to identify crop disease. Followed by, the farmers are updated with the results from disease diagnosis. The system functions based on three dimensions, such as fine-grained disease, coarse-grained disease, and species. All these dimensional results are fused by the compensation algorithm present in the compensation layer.

4.5.5 | SCA-based RideNN

In this scheme, the nodes are deployed above the simulation environment to capture the images of plant leaves. This scheme maintains a sink node when the information is collected via an automated plant disease detection module and aids in IoT-based monitoring. Then, the median filter is used to preprocess the images from these nodes to make it compatible with the plant disease detection process. Image segmentation is then executed, which extracts pixel level and segment level features from the source image. Followed by, SCA-based RideNN is utilized in the classification of disease detection.

4.5.6 | Proposed Taylor-WWO-based GAN

The current research work makes use of Taylor-WWO-based GAN for disease identification in agriculture.

(a) Analysis by varying training data

In Figure 11, the author portrays the results attained from the compared methods using training data in terms of accuracy, sensitivity, and specificity parameters. Figure 11A shows the accuracy analysis of various methods. For 50% training data, the accuracy values of the methods, like, MFCN, Deep learning-NN, CNN, MDFC–ResNet, SCA-based RideNN, and proposed Taylor-WWO-based GAN were 0.629, 0.336, 0.681, 0.580, 0.685, and 0.689, respectively.

When 90% training data was used, the accuracy values of the methods, like, MFCN, Deep learning-NN, CNN, and proposed Taylor-WWO-based GAN were 0.645, 0.782, 0.840, 0.885, 0.885, and 0.916, respectively. Figure 11B shows the sensitivity analysis of different methods. When 50% training data was used, the sensitivity values of the methods, such as MFCN, Deep learning-NN, CNN, MDFC–ResNet, SCA-based RideNN, and the proposed Taylor-WWO-based GAN are 0.532, 0.270, 0.618, 0.451, 0.611, and 0.604, respectively.

Likewise, for 90% training data, the sensitivity values of the methods, such as MFCN, Deep learning-NN, CNN, MDFC–ResNet, SCA-based RideNN, and the proposed Taylor-WWO-based GAN are 0.620, 0.738, 0.833, 0.824, 0.843, and 0.850, respectively. Figure 11C portrays the specificity analysis on different methods. In the case of 50% training data, the

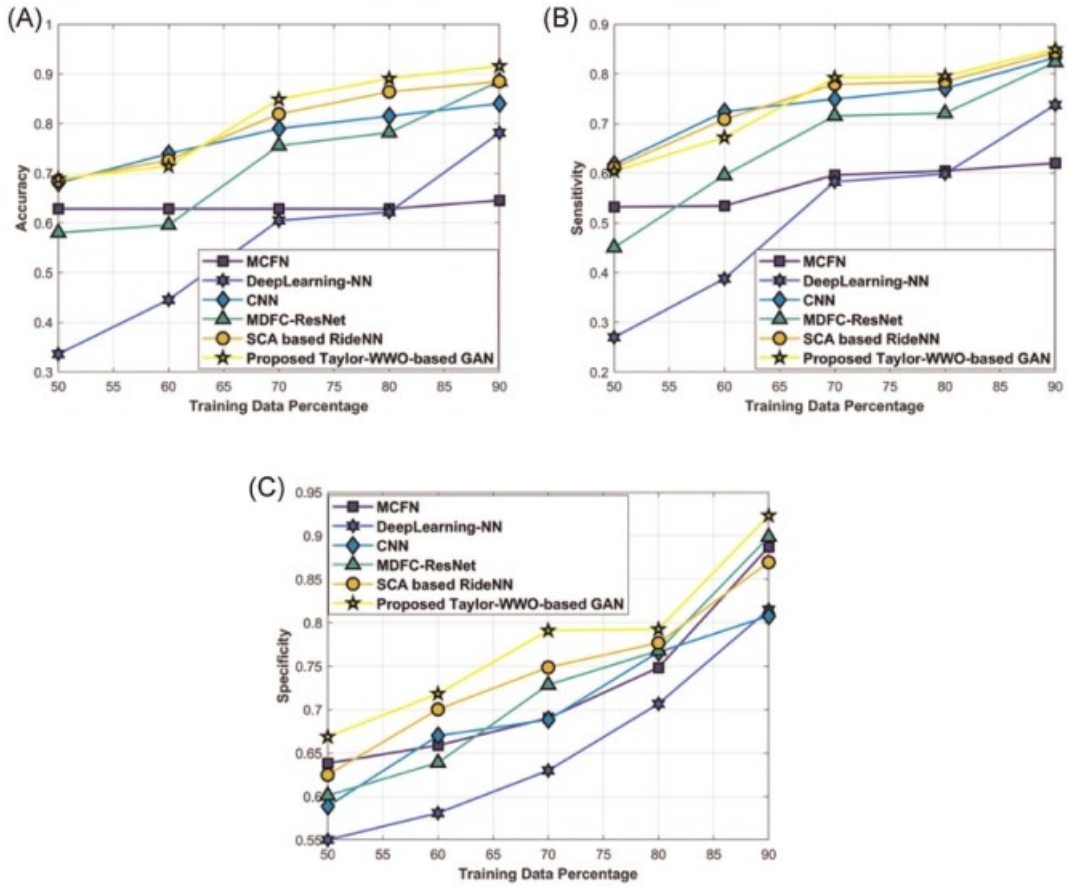

FIGURE 11 Analysis of methods with varying training data using: (A) accuracy, (B) sensitivity, and (C) specificity. CNN, Convolution Neural Networks; GAN, Generative Adversarial Network; MCFN, MultiContext Fusion Network; MDFC, Multidimensional Feature Compensation; NN, Neural Networks; ResNet, Residual Neural Network; SCA, Sine Cosine Algorithm; WWO, Water Wave Optimization [Color figure can be viewed at wileyonlinelibrary.com]

specificity values of the methods, such as MFCN, Deep learning-NN, CNN, and the proposed Taylor-WWO-based GAN were 0.638, 0.550, 0.589, 0.601, 0.625, and 0.669, respectively. The specificity values of the methods, such as MFCN, Deep learning-NN, CNN, and the proposed Taylor-WWO-based GAN for 90% training data were 0.887, 0.815, 0.808, 0.899, 0.869, and 0.923, respectively.

(b) Analysis by varying number of rounds

Figure 12 plots the energy and throughput rates by varying the number of rounds. Figure 12A shows the analysis with an energy parameter. At 200 rounds, the energy values computed by ABC+ACO, FABC +EACO, FGGWO, and FGSA+FGGWO were 0.433, 0.443, 0.447, and 0.448, respectively. Likewise, at 1000 rounds, the energy values computed by ABC+ACO, FABC +EACO, FGGWO, and FGSA+FGGWO were 0.167, 0.183, 0.205, and 0.216, respectively. Figure 12B shows the analysis results with the throughput rate parameter. At 200 rounds, the throughput rates computed by ABC+ACO, FABC+EACO, FGGWO, and FGSA+FGGWO were 0.903, 0.950, 0.950, and 0.950, respectively. As earlier, during 1000

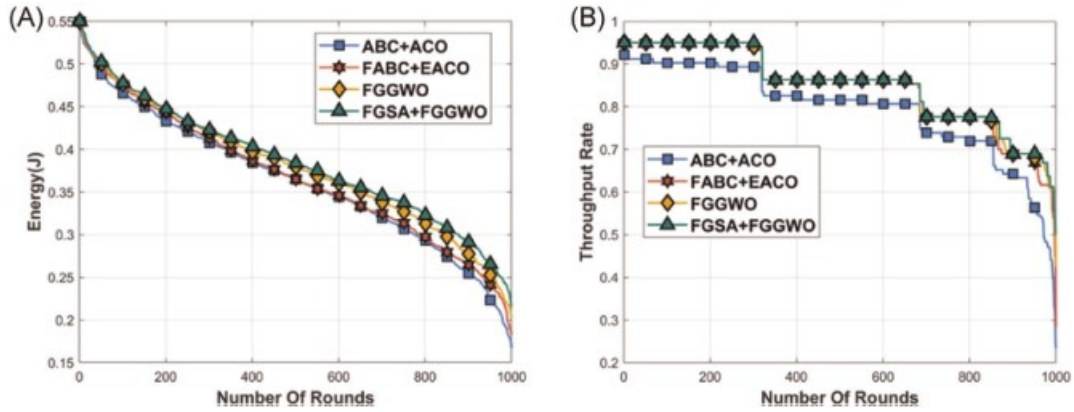

FIGURE 12 Analysis of methods with varying rounds using: (A) energy and (B) throughput rate. ABC, Artificial Bee Colony; ACO, Ant Colony Optimization; EACO, efficient ant colony optimization; FABC, fully informed artificial bee colony; FGGWO, Fractional Gravitational Gray Wolf Optimization; FGSA, fuzzy gravitational search algorithm [Color figure can be viewed at wileyonlinelibrary.com]

rounds, the throughput rates computed by ABC+ACO, FABC+EACO, FGGWO, and FGSA+FGGWO were 0.234, 0.283, 0.425, and 0.500, respectively.

(c) Analysis using cross-validation

Cross-validation is a prevailing defensive measure against overfitting. Using the cross-validation, the hyperparameters of the model are tuned with only the original training set. This allows one to keep the test set as a truly unseen data set for selecting the final model. Cross-validation splits the training and testing set repeatedly. Using the initial training data, multiple mini train-test splits are generated. Then, these splits are used to tune the model. In standard k-fold cross-validation, the data are partitioned into k subsets, called folds. Then, the model is trained iteratively on k − 1 folds while using the remaining fold as the test set.

Figure 13 shows the results attained from the compared methods using cross-validation in terms of accuracy, sensitivity, and specificity parameters. Figure 13A shows the accuracy analysis of various methods. When k =6, the accuracy values of the methods, like, MFCN, Deep learning-NN, CNN, MDFC–ResNet, SCA-based RideNN, and proposed Taylor-WWO-based GAN are 0.611, 0.637, 0.658, 0.669, 0.679, and 0.738, respectively. When k =10, the accuracy values of the methods, such as MFCN, Deep learning-NN, CNN, and proposed Taylor-WWO-based GAN are 0.811, 0.834, 0.847, 0.876, 0.885, and 0.898, respectively. Figure 13B shows the sensitivity analysis of different methods. When k =7, the sensitivity values of the methods, such as MFCN, Deep learning-NN, CNN, MDFC–ResNet, SCA-based RideNN, and the proposed Taylor-WWO-based GAN are 0.561, 0.531, 0.603, 0.604, 0.656, and 0.725, respectively. Likewise, when k =9, the sensitivity values of the methods, such as MFCN, Deep learning-NN, CNN, MDFC–ResNet, SCA-based RideNN, and the proposed Taylor-WWO-based GAN are 0.724, 0.694, 0.809, 0.819, 0.841, and 0.845, respectively. Figure 13C portrays the specificity analysis on different methods. When k =6, the specificity values of the methods, such as MFCN, Deep learning-NN, CNN, and the proposed Taylor-WWO-based GAN are0.601, 0.604, 0.624, 0.626, 0.650, and 0.682, respectively. The specificity values of the methods, such as MFCN, Deep learning-NN, CNN, and the proposed Taylor-WWO-based GAN when k =10 are0.776, 0.832, 0.846, 0.883, 0.898, and 0.909, respectively.

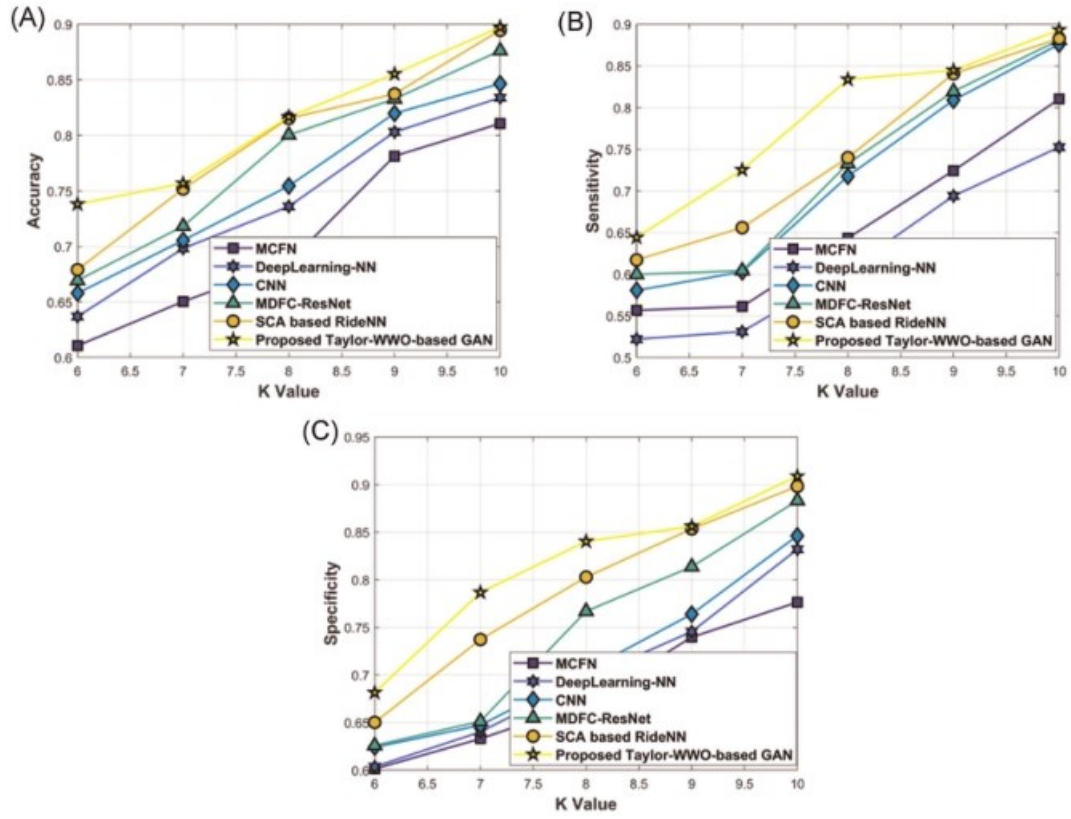

FIGURE 13 Analysis of methods using cross-validation: (A) accuracy, (B) sensitivity, and (C) specificity. CNN, Convolution Neural Networks; GAN, Generative Adversarial Network; MCFN, MultiContext Fusion Network; MDFC, Multidimensional Feature Compensation; NN, Neural Networks; ResNet, Residual Neural Network; SCA, Sine Cosine Algorithm; WWO, Water Wave Optimization [Color figure can be viewed at wileyonlinelibrary.com]

4.6 | Comparative discussion

The methods were analyzed to showcase the effectiveness of the proposed Taylor-WWO-based GAN using accuracy, sensitivity, and specificity parameters. In addition, both energy and throughput rate graphs were plotted with varying numbers of iterations.

(a) Analysis with training data

Table 2 describes the accuracy, sensitivity, and specificity evaluation analysis of various techniques using different training data. The proposed Taylor-WWO-based GAN accomplished the maximum accuracy of 0.916, whereas the accuracy values attained by MFCN, Deep learning-NN, CNN, MDFC–ResNet, SCA-based RideNN were 0.645, 0.782, 0.840, 0.885, and 0.885. With the accuracy parameter, the performance improvement of the proposed Taylor-WWO-based GAN compared to MFCN was 29.585%. The proposed Taylor-WWO-based GAN achieved the maximum sensitivity of 0.850, whereas the sensitivity values achieved by MFCN, Deep learning-NN, and CNN were 0.620, 0.738, and 0.833. With sensitivity parameter, the performance improvement of the proposed Taylor-WWO-based GAN, compared to MFCN, was 27.058%. The maximum specificity of 0.923 was achieved by the proposed Taylor-WWO-based

TABLE 2 Analysis of the methods with training data

Metrics	MFCN	Deep learning-NN	CNN	MDFC–ResNet	SCA-based RideNN	Proposed Taylor-WWO-based GAN
Accuracy	0.645	0.782	0.840	0.885	0.885	0.916
Sensitivity	0.620	0.738	0.833	0.824	0.843	0.850
Specificity	0.887	0.815	0.808	0.899	0.869	0.923

Abbreviations: CNN, Convolution Neural Networks; GAN, Generative Adversarial Network; MCFN, MultiContext Fusion Network; MDFC, Multidimensional Feature Compensation; NN, Neural Networks; ResNet, Residual Neural Network; SCA, Sine Cosine Algorithm; WWO, Water Wave Optimization.

TABLE 3 Analysis of the methods with rounds

Metrics	ABC+ ACO	FABC+EACO	FGGWO	FGSA+FGGWO
Energy	0.167	0.183	0.205	0.216
Throughput rate	0.234	0.283	0.425	0.500

Abbreviations: ABC, Artificial Bee Colony; ACO, Ant Colony Optimization; EACO, efficient ant colony optimization; FABC, fully informed artificial bee colony; FGGWO, Fractional Gravitational Gray Wolf Optimization; FGSA, fuzzy gravitational search algorithm.

GAN, whereas the specificity values computed by MFCN, Deep learning-NN, and CNN were 0.887, 0.815, and 0.808. With specificity parameter, the performance improvement of the proposed Taylor-WWO-based GAN, compared to MFCN, was 3.900%.

The results attained from the analysis established the supremacy of the presented Taylor-WWO-based GAN in detecting plant disease. A significant improvement was observed in the training capability of the proposed algorithm, thanks to the incremental behavior of the optimization algorithm in deep learning. The results infer that the presented Taylor-WWO-based GAN can enhance prediction accuracy and get rid of the overfitting problem. The accuracy got improved since the current research work combined GAN and Taylor-WWO in contrast to existing approaches that used only GAN. GAN can produce high-resolution labeled images and can grasp the hierarchy of representations from a wide range of image data sets. With this added advantage, the proposed technique attained excellent results in contrast to traditional methods.

(b) Analysis with number of rounds

Table 3 displays the analysis of methods by varying the number of rounds. Here, energy and throughput rate graphs were plotted against varying number of iterations. The maximal energy of 0.216 was accomplished by FGSA+FGGWO, whereas the energy values achieved by ABC+ACO, FABC+EACO, and FGGWO were 0.167, 0.183, and 0.205. The maximal throughput rate, that is, 0.500 was accomplished by FGSA+FGGWO, whereas the throughput rates of ABC+ACO, FABC+EACO, and FGGWO were 0.234, 0.283, and 0.425. Hence, the analysis reveals that the combination of FGSA+FGGWO achieved an improvement in energy and throughput rate. It is also found to be suitable for effective routing and determining effective paths.

It is precise from the discussion made above that the proposed technique accomplished

superior performance in comparison with traditional methods. The proposed method gained a

TABLE 4 Analysis of the methods using cross-validation

Metrics	MFCN	Deep learning-NN	CNN	MDFC–ResNet	SCA-based RideNN	Proposed Taylor-WWO-based GAN
Accuracy	0.811	0.834	0.847	0.876	0.885	0.898
Sensitivity	0.810	0.753	0.876	0.881	0.883	0.893
Specificity	0.776	0.832	0.846	0.883	0.898	0.909

Abbreviations: CNN, Convolution Neural Networks; GAN, Generative Adversarial Network; MCFN, MultiContext Fusion Network; MDFC, Multidimensional Feature Compensation; NN, Neural Networks; ResNet, Residual Neural Network; SCA, Sine Cosine Algorithm; WWO, Water Wave Optimization.

significant level of training capability since the optimization technique gained excellent insights during deep learning. On the basis of FGGWO, the optimum path was selected to transmit the information to BS. The combined FGSA+FGGWO method is highly advantageous, thanks to the combination of both techniques. It provides different paths to transmit the information using convergence, and it can function in the presence of multiple constraints too. These unique characteristics helped in achieving the best results.

(c) Analysis using cross-validation

Table 4 describes the accuracy, sensitivity, and specificity of various techniques using cross-validation based on the best performance. The proposed Taylor-WWO-based GAN obtained the maximum accuracy of 0.898, whereas the accuracy values attained by MFCN, Deep learning-NN, CNN, MDFC–ResNet, SCA-based RideNN are 0.811, 0.834, 0.847, 0.876, and 0.885, respectively. The proposed Taylor-WWO-based GAN achieved the maximum sensitivity of 0.893, whereas the sensitivity values achieved by MFCN, Deep learning-NN, CNN, MDFC–ResNet, SCA-based RideNN are 0.810, 0.753, 0.876, 0.881, and 0.883, respectively. The maximum specificity of 0.909 is achieved by the proposed Taylor-WWO-based GAN, whereas the specificity values computed by MFCN, Deep learning-NN, CNN, MDFC–ResNet, SCA-based RideNN are 0.776, 0.832, 0.846, 0.883, and 0.898, respectively.

5 | CONCLUSION

This paper devised a novel method, that is, Taylor-WWO-based GAN for disease identification using an IoT network. In this method, the IoT nodes sensed the plant leaves, whereas the sensed data was transmitted to BS using FGGWO. This FGGWO selected the best path for data transmission. Thus, the routing was performed using an IoT network. After IoT routing, crop diseases were identified at BS. For detecting crop diseases, the input image acquired from the IoT routing phase was subjected to preprocessing to improve the quality of the image. Then, SegNet was adapted to segment the images, and the feature extraction was performed with the acquired segments. The extracted features were then employed by GAN, trained by the Taylor-WWO algorithm. The proposed Taylor-WWO was developed by integrating the Taylor series and WWO algorithm. The proposed Taylor-WWO-based GAN exhibited improved performance with maximum accuracy, sensitivity, and specificity values of 91.6%, 89.3%, and 92.3%, respectively. In the future, advanced deep learning methodologies can be adapted to improve the crop disease detection process. Also, the data set for training can be gathered from various sources with various cultivations, image capturing modes, and geographical areas.

REFERENCES

1. Novikov DA. Systems theory and systems analysis. Systems engineering. In: Cybernetics. Studies in Systems, Decision and Control, Vol 47. Cham: Springer; 2016. https://doi.org/10.1007/978-3-319-27397-6_4
2. Jimeneza A-F, Cardenas P-F, Canales A, Jimenez F, Portacio A. A survey on intelligent agents and multi-agents for irrigation scheduling. Comput Electron Agric. 2020;176:105474. https://doi.org/10.1016/j.compag.2020.105474
3. Russell SJ, Norvig P. Artificial Intelligence: a Modern Approach. 2nd ed. Upper Saddle River, NJ: Prentice Hall; 2003. Chapter 2. ISBN 0-13-790395-2.
4. Wadhawan VK. Robots of the future. Reson. 2007;12:61-78. https://doi.org/10.1007/s12045-007-0073-7
5. Jimenezb A-F, Cardenas P-F, Jimenez F, Ruiz-Canales A, López A. A cyber-physical intelligent agent for irrigation scheduling in horticultural crops. Comput Electron Agric. 2020;178:105777. https://doi.org/10.1016/j.compag.2020.105777
6. UN, n.d. Top 10 countries population [WWW Document]. https://d32ogoqmya1dw8.cloudfront.net/images/integrate/teaching_materials/water_science_society/student_materials/top_10_countries_population.png. Accessed August 18, 2020.
7. India Brand Equity Foundation (IBEF). Agriculture in India: Information about Indian Agriculture & Its Importance. IBEF-Department of Commerce, Ministry of Commerce and Industry, Government of India; 2020. https://www.ibef.org/industry/agriculture-india.aspx
8. Research ZM. Global Smart Agriculture Market Will Reach USD 15,344 million by 2025: Zion Market Research [WWW Document]. 2018. https://www.globenewswire.com/news-release/2018/03/22/1444017/0/en/Global-Smart-Agriculture-Market-Will-Reach-USD-15-344-million-by-2025-Zion-Market-Research. html?print=1. Accessed August 18, 2020.
9. Digiteum, n.d. Is IoT the Future of Agriculture? [WWW Document]. https://www.digiteum.com/iot-agriculture. Accessed August 18, 2020.
10. Andrew M. Smart Farming in 2020: How IoT sensors are creating a more efficient precision agriculture industry [WWW Document]. 2020. https://www.businessinsider.com/smart-farming-iot-agriculture?IR=T. Accessed August 18, 2020.
11. Jeff D. This animation compares the population growth of India and China. World Economic Forum, 99-93 route de la capite, ch-1223. 2017. https://www.weforum.org/agenda/2017/08/this-animation-compares-the-population-growth-of-india-and-china
12. Architectural Documentaries. World Population 1800-2050 [WWW Document]. 2016. http://archidocu.com/wp-content/uploads/2016/12/World-Population-1800-2050.jpg. Accessed August 18, 2020.
13. Singh V, Misra AK. Detection of plant leaf diseases using image segmentation and soft computing techniques. Inf Process Agric. 2017;4:41-49. https://doi.org/10.1016/j.inpa.2016.10.005
14. Cropin, n.d. What is IoT?— The simple explanation [WWW Document]. https://www.cropin.com/iot-internet-of-things-applications-agriculture/. Accessed August 18, 2020.
15. Ramesh S, Rajaram B. IoT based crop disease identification system using optimization techniques. ARPN J Eng Appl Sci. 2018;13:1392-1395.
16. Sharma R, Kamble SS, Gunasekaran A, Kumar V, Kumar A. A systematic literature review on machine learning applications for sustainable agriculture supply chain performance. Comput Oper Res. 2020;119:104926. https://doi.org/10.1016/j.cor.2020.104926

17. Thorat A, Kumari S, Valakunde ND. An IoT based smart solution for leaf disease detection. In: 2017 International Conference on Big Data, IoT and Data Science (BID). Pune: IEEE; Vol 13, 2017:193-198. https://doi.org/10.1109/BID.2017.8336597
18. Wahabzada M, Mahlein A-K, Bauckhage C, Steiner U, Oerke E-C, Kersting K. Plant phenotyping using probabilistic topic models: uncovering the hyperspectral language of plants. Sci Rep. 2016;6:22482. https://doi.org/10.1038/srep22482
19. Khattab A, Habib S, Ismail H, Zayan S, Fahmy Y, Khairy M. An IoT-based cognitive monitoring system for early plant disease forecast. Comput Electron Agric. 2019;166:105028. https://doi.org/10.1016/j.compag.2019.105028
20. Khatua PK, Ramachandaramurthy VK, Kasinathan P, Yong JY, Pasupuleti J, Rajagopalan A. Application and assessment of internet of things toward the sustainability of energy systems: challenges and issues. Sustain Cities Soc. 2020;53:101957. https://doi.org/10.1016/j.scs.2019.101957
21. Zhao Y, Liu L, Xie C, et al. An effective automatic system deployed in agricultural Internet of things using multi-context fusion network towards crop disease recognition in the wild. Appl Soft Comput. 2020;89: 106128-106597. https://doi.org/10.1016/j.asoc.2020.106128
22. Mohammed HR. Mapping paddy rice fields using landsat and sentinel radar images in urban areas for agriculture planning. J Plan Dev. 2020;41:1-28.
23. Shende V, Mahendra P. IoT based preventive crop disease model using IP and CNN. Int Res J Eng Technol. 2019;6:1270-1272.
24. Alonso RS, Sittón-Candanedo I, García Ó, Prieto J, Rodríguez-González S. An intelligent Edge-IoT platform for monitoring livestock and crops in a dairy farming scenario. Ad Hoc Networks. 2020;98:102047. https://doi.org/10.1016/j.adhoc.2019.102047
25. Wolfert S, Goense D, Sørensen CAG. A future internet collaboration platform for safe and healthy food from farm to fork. In: 2014 Annual SRII Global Conference. San Jose, USA: IEEE; 2014:266-273. https://doi.org/10.1109/SRII.2014.47
26. Pujari JD, Yakkundimath R, Byadgi AS. Image processing based detection of fungal diseases in plants. Procedia Comput Sci. 2015;46:1802-1808. https://doi.org/10.1016/j.procs.2015.02.137
27. Gupta AK, Gupta K, Jadhav J, Deolekar RV, Nerurkar A, Deshpande S. Plant disease prediction using deep learning and IoT. In: 2019 6th International Conference on Computing for Sustainable Global Development (INDIACom). New Delhi, India: IEEE; 2019:902-907.
28. Atole RR, Park D. A multiclass deep convolutional neural network classifier for detection of common rice plant anomalies. Int J Adv Comput Sci Appl. 2018;9:67-70.
29. Li D, Wang R, Xie C, et al. A recognition method for rice plant diseases and pests video detection based on deep convolutional neural network. Sensors. 2020;20:578. https://doi.org/10.3390/s20030578
30. Abu Bakar MN, Abdullah AH, Abdul Rahim N, Yazid H, Misman SN, Masnan MJ. Rice leaf blast disease detection using multi-level colour image thresholding. J Telecommun Electron Comput Eng. 2018;10:1-6.
31. Chawal B, Panday S. Rice plant disease detection using twin support vector machine (TSVM). J Sci Eng. 2019;7:61-69. https://doi.org/10.3126/jsce.v7i0.26794
32. Hu R, Xu H, Rohrbach M, Feng J, Saenko K, Darrell T. Natural language object retrieval. In: 2016 IEEE Conference on Computer Vision and Pattern Recognition (CVPR), Las Vegas, NV, USA. 2016:4555-4564. https://doi.org/10.1109/CVPR.2016.493
33. Dang KB, Burkhard B, Windhorst W, Müller F. Application of a hybrid neural-fuzzy inference system for mapping crop suitability areas and predicting rice yields. Environ Model Software. 2019;114:166-180. https://doi.org/10.1016/j.envsoft.2019.01.015
34. Dhumane AV, Prasad RS. Fractional gravitational grey wolf optimization to multi-path data transmission in IoT. Wirel Pers Commun. 2018;102:411-436. https://doi.org/10.1007/s11277-018-5850-y
35. Jiang F, Gong M, Zhan T, Fan X. A semi supervised GAN-based multiple change detection framework in multi-spectral images. IEEE Geosci Remote Sens Lett. 2020;17:1223-1227. https://doi.org/10.1109/LGRS.2019.2941318
36. Mishra M, Choudhury P, Pati B. Modified ride-NN optimizer for the IoT based plant disease detection. J Ambient Intell Hum Comput. 2020;12:691-703. https://doi.org/10.1007/s12652-020-02051-6
37. Chalapathy R, Chawla S. Deep Learning for Anomaly Detection: a Survey. 2019. preprint arXiv:1901.03407.

38. Chaki J, Parekh R. Plant leaf recognition using shape based features and neural network classifiers. Int J Adv Comput Sci Appl. 2011;2:41-47. https://doi.org/10.14569/IJACSA.2011.021007
39. Amara J, Bouaziz B, Algergawy A. A deep learning-based approach for banana leaf diseases classification. In: Mitschang B, Nicklas D, Leymann F, et al., eds. Datenbanksysteme Für Business, Technologie Und Web (BTW 2017)—Workshopband. Bonn: Gesellschaft für Informatik e.V.; 2017:79-88.
40. Zhong L, Hu L, Zhou H. Deep learning based multi-temporal crop classification. Remote Sens Environ. 2019;221:430-443. https://doi.org/10.1016/j.rse.2018.11.032
41. Richey B, Majumder S, Shirvaikar M, Kehtarnavaz N. Real-time detection of maize crop disease via a deep learning-based smartphone app. In: Proceedings of the SPIE. SPIE digital library; 2020. https://doi.org/10.1117/12.2557317
42. Rodríguez L, Castillo O, García M, Soria J. A new randomness approach based on sine waves to improve performance in metaheuristic algorithms. Soft Comput. 2020;24:11989-12011. https://doi.org/10.1007/s00500-019-04641-9
43. Rodríguez L, Castillo O, Soria J, et al. A fuzzy hierarchical operator in the grey wolf optimizer algorithm. Appl Soft Comput. 2017;57:315-328. https://doi.org/10.1016/j.asoc.2017.03.048
44. Rodríguez L, Castillo O, García M, Soria J. Constrained real-parameter optimization using the firefly algorithm and the grey wolf optimizer. In: Castillo O, Melin P, eds. Hybrid Intelligent Systems in Control, Pattern Recognition and Medicine. Studies in Computational Intelligence. Vol 827. Cham: Springer; 2019:155-167. https://doi.org/10.1007/978-3-030-34135-0_11
45. Sanchez DF, Melin P, Castillo O. A grey wolf optimizer for modular granular neural networks for human recognition. Comput Intell Neurosci. 2017;8:1-26. https://doi.org/10.1155/2017/4180510
46. Badrinarayanan V, Kendall A, Cipolla R. SegNet: a deep convolutional encoder–decoder architecture for image segmentation. IEEE Trans Pattern Anal Mach Intell. 2017;39:2481-2495. https://doi.org/10.1109/TPAMI.2016.2644615
47. Largeron C, Moulin C, Géry M. Entropy based feature selection for text categorization. Proceedings of the 2011 ACM Symposium on Applied Computing (SAC '11). New York, NY, USA: ACM; 2011:924-928. https://doi.org/10.1145/1982185.1982389
48. Jun B, Choi I, Kim D. Local transform features and hybridization for accurate face and human detection. IEEE Trans Pattern Anal Mach Intell. 2013;35:1423-1436.
49. Gao Y, Kong B, Mosalam KM. Deep leaf-bootstrapping generative adversarial network for structural image data augmentation. Comput Civ Infrastruct Eng. 2019;34:755-773. https://doi.org/10.1111/mice.12458
50. Pascual S, Bonafonte A, Serrà J. {SEGAN:} Speech enhancement generative adversarial network. CoRR. 2017. abs/1703.0.
51. AlameluMangai S, Sankar BR, Alagarsamy K. Taylor series prediction of time series data with error propagated by artificial neural network. Int J Comput Appl. 2014;89:41-47. https://doi.org/10.5120/15470-4112
52. Zheng Y-J. Water wave optimization: a new nature-inspired metaheuristic. Comput Oper Res. 2015;55:1-11. https://doi.org/10.1016/j.cor.2014.10.008
53. Prajapati H, Shah J, Dabhi V. Rice leaf diseases data set. Intell Decis Technol. 2017;11:357-373. https://doi.org/10.3233/IDT-170301
54. Hu W-J, Fan J, Du Y-X, Li B-S, Xiong N, Bekkering E. MDFC–ResNet: an agricultural IoT system to accurately recognize crop diseases. IEEE Access. 2020;8:115287-115298. https://doi.org/10.1109/ACCESS.2020.3001237